

Exploiting Redundancy to Reduce Impact Force*

Matthew Wayne Gertz**, Jin-Oh Kim†, and Pradeep K. Khosla‡

Advanced Manipulators Laboratory
The Robotics Institute
Carnegie Mellon University
Pittsburgh, Pennsylvania 15213

Abstract

This paper presents strategies for reducing the impact force resulting from the collision of a kinematically redundant manipulator with an object in its environment. The Premultiplier Diagram, a tool used to derive the impact force reduction strategies presented in this paper, is introduced and discussed. Two strategies for reducing impact force are then presented. The first strategy involves adding torques to the joints of the redundant manipulator to impede motion into the object with which it collides. The second strategy involves choosing the best configuration for the impact event. Simulated results from the testing of either strategy are presented and discussed.

1. Introduction

There has been much research in the past decade on the use of kinematically redundant manipulators [11][8][13]. Recently, research has been performed on how redundancy can be used to minimize the force of impact between the end-effector of a manipulator and an object [1][5][12][10][3]. Minimization of the impact force is important, since expensive and hard-to-replace end-effectors can be damaged by excessive force. A redundant manipulator has an advantage over a non-redundant manipulator for minimizing the force of impact, since it is capable of contacting a surface in an infinite number of configurations. Since different configurations have different attributes (such as effective mass, effective damping, and effective stiffness in task space), it stands to reason that by altering the configuration, we alter how the manipulator responds during impact. Similarly, since we can alter the joint configuration of a redundant manipulator without causing its end-effector to move, we can apply torques which impede motion into the object without affecting joint motions which do not contribute to object penetration. This paper addresses both ideas for minimizing impact force.

Past work on impact strategies has focused on the instantaneous effects of impact, where the duration of the impact occurs in an infinitesimally small period of time. Walker [10] showed that reducing the instantaneous force of impact can be accomplished by minimizing the effective mass of the redundant manipulator. Zheng and Hemami [12] explored the relationship between abrupt changes in generalized joint rate velocities and the intensity of collision during an instantaneous impact event. Cai [1] provided a method for determining the im-

pulse of a perfectly elastic collision having a duration that is less than the controller's sampling period. Khatib and Burdick [5] modeled the impact event as non-instantaneous, but only for a non-redundant manipulator. The theories presented in this paper differ from these previous theories in that we model the impact event as having some finite duration for a redundant manipulator. Assuming that the environment can be modeled as ideal springs of some constant stiffness, then the impact force experienced at the end-effector is the product of the stiffness of the object and the distance the object is compressed (referred to as "penetration"). It is clear that minimizing penetration minimizes the impact force [3], and so our strategies focus on minimizing the penetration of the end-effector into the object.

In Section 2, we will present the Premultiplier Diagram, a tool which we will use to construct our impact force minimization strategies. Section 3 introduces the first minimization strategy, which involves adding torques to the joints of the redundant manipulator to impede motion into the object (impact control). In Section 4, we give our second strategy, which minimizes impact force by choosing the best configuration for impact (impact planning). Section 5 shows and discusses the results under simulation from the testing of both methods. In Section 6, we conclude this paper.

2. The Premultiplier Diagram

2.1. Dynamics of Redundant Manipulators

The dynamic motion of an n degrees-of-freedom (DOF) manipulator can be modeled as:

$$\tau = H(\theta) + C(\theta, \dot{\theta}) + G(\theta) \quad (1)$$

where C and G represent the $(n \times 1)$ Coriolis/centrifugal and gravitational force vectors, and τ and θ are $(n \times 1)$ joint torque and angle vectors in joint space, respectively. The matrix H is an $(n \times n)$ inertia matrix. The corresponding equation of the end-effector motion in an m -dimensional operational space can be written as [5]:

$$F = M(\theta) \ddot{P} + B(\theta, \dot{\theta}) + Q(\theta) \quad (2)$$

where B and Q are the $(m \times 1)$ Coriolis/centrifugal and the gravitational forces in the operational space and F is an $(m \times 1)$ generalized operational force vector. The vector P is an independent $(m \times 1)$ operational parameter.

The relationship between τ and F is:

$$\tau = J^T F \quad (3)$$

where J is the $(n \times m)$ Jacobian matrix. This equation implies that there exists a joint torque τ corresponding to an operational force F . However, the opposite does not apply in general, especially for a redundant manipulator, for which the joint torque given by (3) controls only the net motion of the end-effector. The relationship between $\dot{\theta}$ and \dot{P} can be obtained by differentiating the instantaneous kinematics ($\dot{P} = J\dot{\theta}$) with respect to time:

$$\ddot{P} = J\ddot{\theta} + \dot{J}\dot{\theta} \quad (4)$$

* This research was funded in part by NASA (grant number NAG-1-1075), the Dept. of Elec. and Comp. Engineering, and The Robotics Institute at Carnegie Mellon University.

** Graduate Student, Ph.D. program, Dept. of Elec. and Comp. Engineering, The Robotics Institute at Carnegie Mellon University.

† Graduate Student, Robotics Ph.D. program, The Robotics Institute at Carnegie Mellon University.

‡ Associate Professor, Department of Electrical and Computer Engineering, Carnegie Mellon University.

The simplest form of the above dynamic equations can be obtained when the joint velocity is zero, the gravitational term is zero, and joints are just about to start moving. Then, the above four equations can be written as:

$$(a) \tau = H\ddot{\theta}, (b) F = M\ddot{P}, (c) \tau = J^T F, \text{ and } \ddot{P} = J\ddot{\theta} \quad (5)$$

These four equations are substituted into Figure 1, and two generalized

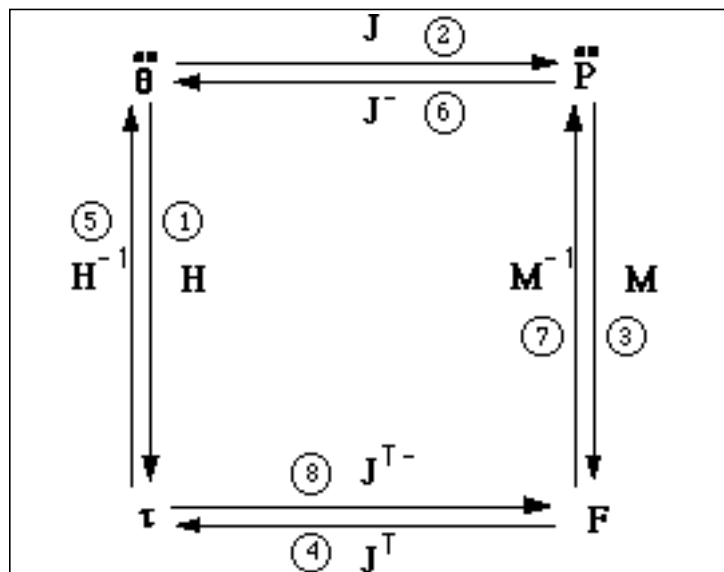


Figure 1: The Dynamic Premultiplier Diagram

inverses (J^{-} and J^{T-}) of J and J^T , respectively, are introduced to define two undetermined paths (6 and 8). This is the dynamic version of the Premultiplier Diagram given in [7]. From this diagram, we can obtain the two generalized inverses (g-inverses) and relationships between inertia matrices (M and H) by the use of circuitous paths. For instance, Path 6 is equivalent to Path 3→4→5, which results in the following:

$$J^{-} = H^{-1} J^T M \quad (6)$$

The left side of (6) is obtained by premultiplying the old path by the new path as we follow the circuitous path. Similarly, we can obtain the following:

$$J^{T-} = M J H^{-1} \quad (7)$$

$$M^{-1} = J H^{-1} J^T \quad (8)$$

$$H = J^T M J \quad (9)$$

The g-inverse J^{-} is the inertia matrix (H) weighted minimum norm g-inverse [9]. Hereafter, J_H^{+} will be used instead to explicitly show the weight used. Since the inertia matrix H is symmetric and positive definite, J^{T-} (J_H^{+T}) is equal to the transpose of J^{-} (J_H^{+}). The g-inverse obtained in (6) provides the optimal and natural decomposition between the net and null motions of a redundant manipulator because the joint torque obtained by the inertia-weighted g-inverse minimizes the interaction between the net and null motions. This implies that the dynamic controller must be based on the inertia-weighted g-inverse to achieve the optimal control. This is a result from the cooperation of dynamics and kinematics of a redundant manipulator. The above four equations (6)-(9) are still valid for nonzero joint velocity. For more detail, refer to [6][7].

2.2. Physics of Impact

The physics of the impact phenomenon between the end-effector and the environment are discussed in this section. Two different impact models exist: first, the case where the impact period is infinitesimally small; second, where the impact period is long enough to be controllable. Roughly speaking, stiff environments cause an almost zero-duration impact period, whereas soft environments cause longer impact periods.

For the first case, the velocity of the manipulator after impact is decided by the velocity before impact, the configuration of the manipulator, and the stiffness of the environment. When the stiffness of

the environment and the velocity before impact are given, the only variable we can control is the configuration of the manipulator before impact. For the second case, the impact period is relatively long enough so that we can actively dissipate the kinetic energy of the manipulator and manipulate the null motion in a direction to reduce the impact force. Thus, variables we can control are the configuration before impact and the damping term of control. In the remainder of this section, the physics of impact for the first case (infinitesimal impact period) are discussed, and in the following two sections, the second case (relatively long impact period) is studied.

The dynamic equations (1) and (2) can be integrated over an infinitesimal time period (Δt):

$$\hat{\tau} = H\Delta\dot{\theta} \text{ and } \hat{F} = M\Delta\dot{P} \quad (10)$$

where $\hat{\tau}$ and \hat{F} are impulse torques and forces, respectively, defined by:

$$\hat{\tau} = \int_0^{\Delta t} \tau dt \text{ and } \hat{F} = \int_0^{\Delta t} F dt \quad (11)$$

The Coriolis/centrifugal and gravitational terms are negligibly small when they are integrated over an infinitesimal time period ($\Delta t \approx 0$). The relationship between $\Delta\dot{\theta}$ and $\Delta\dot{P}$ is the same as (3) for dynamics, since the Jacobian matrix can be assumed as constant over the infinitesimal time period. The relationship between $\Delta\dot{\theta}$ and $\Delta\dot{P}$ is obtained by integrating (4) as:

$$\Delta\dot{P} = J\Delta\dot{\theta} \quad (12)$$

These relationships are substituted into the Impact Premultiplier Diagram in Figure 2, which is the integrated version of the Dynamic Premultiplier Diagram in Figure 1. The diagram helps understand the impact physics and also provides a natural solution of the joint velocity after impact. From this diagram, by the use of Path 6 = Path 3→4→5, we can derive the velocity change in joint space in terms of the velocity change of the end-effector in operational space:

$$\Delta\dot{\theta} = \dot{\theta}_f - \dot{\theta}_i = H^{-1} J^T M \Delta\dot{P} = J^{-} \Delta\dot{P} \quad (13)$$

where the subscripts i and f mean before and after impact, respectively. The same expression of (13) in [1] and [12] proves the correctness of the result found by the use of

the Impact Premultiplier Diagram. The matrix J^{-} in (13) equals the inertia-weighted g-inverse J_H^{+} in (6). This proves that the inertia-weighted g-inverse provides a natural solution for the dynamic resolution of a redundant motion. Equation (13) can be rewritten as:

$$\Delta\dot{\theta} = J_H^{+} \Delta\dot{P} \quad (14)$$

The relationship between impulse force and velocity change in (10) shows that the impulse force can be reduced by choosing joint angles (θ) which minimize the effective mass M . Then the problem can

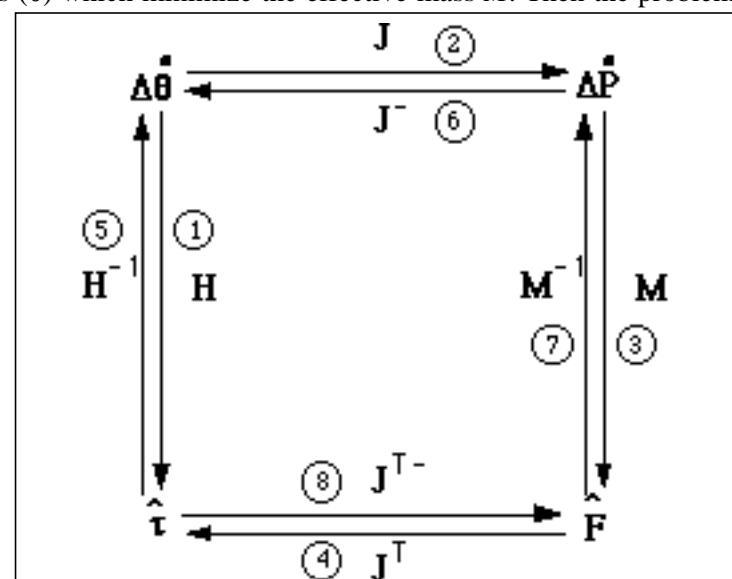


Figure 2: The Impact Premultiplier Diagram

be stated as thus: to derive the best configuration θ before impact, which minimizes the impulse force during impact, assuming that $\Delta\dot{P}$

is given [10]. If the impact happens in the u direction, the impulse force can be minimized by obtaining the configuration of a manipulator which minimizes m_u . The parameter m_u can be obtained as:

$$m_u = u^T M u \quad (15)$$

3. Using Correcting Torques to Minimize Impact Force

3.1. Introduction

With the proper tools to define manipulator properties mathematically given in Section 2 in the form of the Premultiplier Diagram, we can now begin to create strategies to reduce the impact force at the end-effector for impact events having some finite duration. In this section, we present a method for reducing the impact force by introducing correcting torques at the joints to minimize penetration into an object during impact, thus minimizing the impact force. This type of strategy is known as an impact control strategy, since it is used to control the manipulator during sudden (and perhaps unplanned) collisions with the environment.

3.2. Basic Assumptions

We will be modeling the impact event for a redundant manipulator that performs tasks in space, where it would be especially beneficial to reduce the impact force. In this model, we will make several initial assumptions. First of all, we assume that objects in the environment can be simulated as springs of various stiffness, so that minimizing penetration into the object will be sufficient for minimizing the impact force. Second, the links of our manipulator will be assumed to be rigid. Finally, we assume that the collision event will have some duration (i.e. it is not instantaneous).

3.3. The Correcting Torque

As seen in Section 2, we can decompose the general motion of a redundant manipulator into net motion (joint motion which moves the end-effector) and null motion (joint motion which leaves the end-effector's position unchanged). Since null motion does not push the end-effector deeper into the object, there is no reason to reduce it. On the other hand, net motion will push the end-effector into the object, and therefore it must be countered in some manner. This implies the addition of some torque to rotate the joints to correct the effects of net motion. Because we do not want the end-effector to be forced deeper into the surface, we require that this torque introduces net motion in the direction opposite of that in which the end-effector is traveling. This torque will be referred to as the correcting torque.

We can introduce correcting torque as a function of the configuration (proportional feedback, or stiffness torque), a function of the joint velocity (derivative feedback, or damping torque) or a combination of the two. Both the stiffness and damping torque terms will have a null component and a net component, which induce null and net motion, respectively. However, we only need to retard net motion, and therefore we need concern ourselves only with introducing net stiffness torque and/or net damping torque. It is not wise to add a null correcting torque, since this puts an extra strain on the actuators for no good reason. We then have two ways to reduce the impact force. First, we can cancel the null component of a stiffness correcting torque, since a high net stiffness torque is sufficient for reducing the impact force, and apply the resulting torque to the system. Second, we can reduce the size of the null component of a damping torque, increase the size of its net component, and apply that torque as well. (Unlike stiffness torque, the null component of the damping torque should not be set to zero, as will be discussed in the next section.)

For this paper, we shall apply a damping torque as our correcting torque.

3.4. The Damping Torque

We will now turn to examining the specifics of the damping

torque added to retard net motion. Rather than canceling its null component, which is unwise (no matter how hard we try to minimize null motion, there will almost always be some null joint velocity, which we will want damped if we wish the system to come to a halt at some point), we will derive the net and null components of torque and scale them in such a way that net damping is increased and null damping is decreased.

First, we should note that we wish the system to stop moving when it reaches its destination. That is, our desired angular velocity is zero. Any torque that we add will be a product of the joint damping matrix and the joint velocity vector, and therefore, the torque that should be added should be:

$$\tau_D = K_D \dot{\theta} = K_D (\dot{\theta}_d - \dot{\theta}) = -K_D \dot{\theta} \quad (16)$$

where K_D is an $n \times n$ matrix of joint damping terms, and τ_D is some damping torque added to the system.

The decomposition of this torque into its net and null redundancy components is given in [6][7] as:

$$\tau_D = J^T J_H^{+T} \tau_D + \left(I - J^T J_H^{+T} \right) \tau_D = \tau_{Dp} + \tau_{Dh} \quad (17)$$

Now, we wish to increase the net damping in order to slow down the forward progress of the manipulator. As mentioned previously, the null damping cannot be zero, because we would eventually like the system to come to a complete stop. (In a non-ideal system this would not be as big of a problem, since null damping would be caused by joint friction. However, there exist systems which have a very low friction coefficient, and the time that it would take the null motion to cease could be quite long in these systems.) Nevertheless, we do not want high null damping, as previously explained, so we must scale down the null component.

With the direction of the net and null vectors supplied by (17), we scale each component of the damping torque, to control the amount applied to the system:

$$\tilde{\tau}_{Dp} = h_1 \tau_{Dp} \quad (18)$$

$$\tilde{\tau}_{Dh} = h_2 \tau_{Dh} \quad (19)$$

$$\tilde{\tau}_D = \tilde{\tau}_{Dp} + \tilde{\tau}_{Dh} \quad (20)$$

where $\tilde{\tau}_{Dp}$ is the scaled net damping torque, $\tilde{\tau}_{Dh}$ is the scaled null damping torque, and $\tilde{\tau}_D$ is the total damping torque to be added.

Because we desire large net damping and low null damping, it follows that h_1 should be much larger than h_2 , since increasing h_1 increases the net damping torque. An increase in the net damping torque causes the net velocity into the wall to decrease, and the resulting decrease in momentum causes the impact force to be reduced.

The values of h_1 and h_2 should be chosen as appropriate for the actuators of the system. For instance, if the value of h_1 is too high, then the torque calculated by this method will be too large for the actuators, and saturation will occur. One immediate advantage of this strategy, however, is that actuators can be used to their best advantage to reduce impact force. With the null torque component (which is useless for reducing impact force) reduced, the net torque component can be increased to larger values approaching that of the saturation value of the actuator, improving the effectiveness of the impact control strategy.

In Section 5.3, we present and discuss the results of this impact control strategy under simulation.

4. Using the Configuration to Minimize the Impact Force

4.1. Introduction

The strategy of the previous section introduced the idea that impact force can be reduced by adding torques to minimize penetration into the surface of the object with which the end-effector collides. We now introduce a method which instead minimizes the impact force by finding the configuration of the manipulator which increases effective damping and reduces effective mass before impact.

Intuitively, there are certain configurations which are less use-

ful than others when a collision occurs. Hitting a surface while in a configuration which causes a large effective mass at the end-effector will not be helpful in reducing the impact force, no matter what control scheme is used. Similarly, a configuration with low effective damping will not be of any use, because momentum into the surface must be damped. In this section we derive a means for deciding which configurations are useful during a collision, in order to find the best possible configuration to minimize impact force. This type of strategy is called an impact planner, since it is a useful strategy for when we plan to make contact with the environment. This is a generalization of [10].

4.2. Basic Assumptions

As in Section 3, a few assumptions will be made. In addition to those previously given, we shall assume that a one-dimensional collision task can be generalized to a two- or three-dimensional case. We can justify this last assumption by choosing our world and object frames such that motion is along only one axis, and orthogonal to the other two axes. We will also assume that the manipulator has negligible null motion (i.e. the joint trajectory is such that all joint motion is contributing to the movement of the end-effector).

4.3. The Configuration-Based Impact Strategy

Assuming, as above, that the gravity in our environment is zero, the motion of the manipulator during impact is modeled, using the symbols defined in Section 2, as [2][3]:

$$\tau = H(\theta) \ddot{\theta} + C(\theta, \dot{\theta}) - J^T F_e \quad (21)$$

where $F_e = K_e dx$ is the force of impact (the product of environmental stiffness and penetration).

We can separate the inertial component of the torque into net term and null terms:

$$\tau = H\ddot{\theta}_p + H\ddot{\theta}_h + C(\theta, \dot{\theta}) - J^T F_e \quad (22)$$

We must determine what the net angular acceleration actually is. To do this, we recall that task space velocity is given by:

$$\dot{x} = J\dot{\theta} + J\ddot{\theta} \quad (23)$$

We can multiply both sides of the equation by the pseudoinverse of the Jacobian, which we get from the Premultiplier Diagram, and then solve for the net angular acceleration. This gives us:

$$\ddot{\theta}_p = J_H^+ \dot{x} - J_H^+ J \ddot{\theta} \quad (24)$$

We are concerned with the net terms only, having separated out the null terms in equation (22). We can substitute (24) into (22) for the net angular acceleration and get:

$$\tau = HJ_H^+ \dot{x} - HJ_H^+ J \ddot{\theta} + H\ddot{\theta}_h + C(\theta, \dot{\theta}) + J^T F_e \quad (25)$$

Without loss of generality, we can define the position of the object as being at $x = 0$, and then, with the definition of F_e given in (21), equation (25) becomes:

$$\tau = HJ_H^+ \dot{x} - HJ_H^+ J \ddot{\theta} + H\ddot{\theta}_h + C(\theta, \dot{\theta}) + J^T K_e x \quad (26)$$

Rearranging this, we get:

$$HJ_H^+ \dot{x} - HJ_H^+ J \ddot{\theta} + H\ddot{\theta}_h + C(\theta, \dot{\theta}) - \tau + J^T K_e x = 0 \quad (27)$$

Equation (27) can be further simplified. We can drop the term relating to null acceleration because we have assumed that there is negligible null motion. We will assume that the change in the Jacobian is negligible, because any one particular joint changes position very little during impact for a sufficiently stiff surface of impact. (Note that this does not mean that we can cancel out the terms relating to Cartesian variables such as x , since they are a function of all joint positions, velocities, and accelerations, not just one). Finally, we note that the centripetal torque terms are dependent on the square of the joint velocities, and the Coriolis torque terms are dependent on the product of two joint velocities. For our simulated manipulators we have arbitrarily chosen terms for the matrix of damping coefficients introduced in equation

(16) that are on the order of 10^2 ($\text{kg}\cdot\text{m}^2/(\text{sec}\cdot\text{rad}^2)$), as shown in Table 1. If we do not wish to saturate the actuators of the manipulator with torques which are too high for them to handle, then the joint velocities responsible for these torques must be made fairly small, on the order of 10^{-1} rad/sec or less. Therefore, the torque from the centripetal and Coriolis terms will be comparatively small with respect to the other torque terms, since the product of two joint velocities will be very small.

Link i	Mass	a_i	d_i	α_i	θ_{i-1}
1	12.0 kg	1.0 m	0	0	θ_1
2	12.0 kg	1.0 m	0	0	θ_2
3	11.04 kg	0.92 m	0	0	θ_3
e-e	0.96 kg	0.08 m			0
$I_1 = \text{diag}(0.0054, 1.0027, 1.0027) \text{ kg}\cdot\text{m}^2/\text{rad}^2$ $I_2 = \text{diag}(0.0054, 1.0027, 1.0027) \text{ kg}\cdot\text{m}^2/\text{rad}^2$ $I_3 = \text{diag}(0.00497, 0.78117, 0.78117) \text{ kg}\cdot\text{m}^2/\text{rad}^2$ $I_{ee} = \text{diag}(0.00019, 0.00061, 0.00061) \text{ kg}\cdot\text{m}^2/\text{rad}^2$					
$K_D = \text{diag}(200, 150, 100) \text{ kg}\cdot\text{m}^2/(\text{sec}\cdot\text{rad}^2)$					

Table 1: Parameters for the simulated 3DOF planar manipulator.

Canceling the aforementioned torque terms from (27), and substituting (16) in for the torque term τ , we are left with:

$$HJ_H^+ \ddot{x} - \tau + J^T K_e x = HJ_H^+ \ddot{x} + K_D \dot{\theta} + J^T K_e x = 0 \quad (28)$$

We can conclude from (28) that the impact event depends upon three parameters: the mass matrix and the mass-weighted generalized inverse of the Jacobian, which are configuration-dependent; the velocity damping matrix, which is fixed; the angular velocity, which is controllable. We can further separate (28) into net and null parts, introduced in the term having angular velocity. Since we have assumed the null motion to be negligible, (28) becomes:

$$HJ_H^+ \ddot{x} + K_D \dot{\theta}_p + J^T K_e x = 0 \quad (29)$$

The net angular velocity is given by using the pseudoinverse of the Jacobian as determined from the Premultiplier Diagram, so that:

$$J_H^+ \dot{x} = \dot{\theta}_p \quad (30)$$

which we can substitute into (29) to get:

$$HJ_H^+ \ddot{x} + K_D J_H^+ \dot{x} + J^T K_e x = 0 \quad (31)$$

Next, we normalize (31) so that the coefficient matrix of the acceleration vector is the identity matrix. To do this, we derive the pseudoinverse of the coefficient matrix of the acceleration from the Premultiplier Diagram:

$$\left(HJ_H^+ \right)^+ = \left(J_H^+ \right)^+ H^+ = JH^{-1} \quad (32)$$

We can then rewrite (32) by multiplying through by the inverse of the coefficient of the first term in the equation, so that we get:

$$\ddot{x} + JH^{-1} K_D J_H^+ \dot{x} + JH^{-1} J^T K_e x = 0 \quad (33)$$

$JH^{-1} J^T$ is the inverse of the effective mass of the manipulator [4], while $JH^{-1} K_D J_H^+$ simply maps terms involving the ratio of damping terms to mass terms from joint space to Cartesian space. For convenience, we simplify (33) as follows:

$$\ddot{x} + A\dot{x} + M^{-1} K_e x = 0 \quad (34)$$

Thus, we have reduced the impact equations to a second-order differential equation in terms of x , which, since we have defined the location of the object as the zero vector, is simply the penetration of the end-effector into the obstacle. Unfortunately, the coefficients of x and its derivatives are matrices, not scalars. However, the coefficients are task space matrices, of size $m \times m$. To solve this small problem, we can certainly define our world and object frames so that the motion of the end-effector is along one of the axes (say, for instance, the x -axis), and orthogonal to the other axes (y and z). Since motion is orthogonal to the y - and z -axes, any coefficients involving terms along those axes do

not contribute to the penetration into the wall in the direction of the x -axis. When we choose our frames this way, (34) becomes (using equation (15)):

$$\ddot{x} + a_x \dot{x} + c_x x = 0 \quad (35)$$

where a_x is the element of A strictly along the vector of motion ($u^T A u$) (sec^{-1}), and c_x is the element of $M^{-1} K_e$ strictly along the vector of motion ($u^T M^{-1} K_e u$) (sec^{-2}). Khatib and Burdick in [5] offer a similar second-order model having $a_x = 0$ (pure oscillation).

We can now find a way to rate configurations based on their ability to damp the net motion, and thus reduce the impact force. Let us assume that the wall is stiff enough so that the poles of (35) are oscillatory. From basic control theory, then, we would deduce that increase the value of a_x in the same equation would decrease the penetration into the object, and therefore the impact force, since the real location of the poles would shift to the left. This has the effect of increasing system damping and decreasing overshoot beyond the object's outer boundary. We would therefore expect that the configuration having the largest value of a_x will globally be the configuration causing the least penetration at impact. The results which show this under simulation are given in Section 5.4.

5. Results from Strategies, under Simulation

5.1. Introduction

In this section, we present the tests performed on the strategies presented in the previous two sections, and discuss the results. The simulator used for these tests was the NASA Langley Robotics Systems Simulator (ROBSIM), which was modified extensively for use in this research [3].

5.2. The Testing Environment

For these tests, we defined the gravity of the environment to be zero, and we allowed the end-effector to have only net motion at the time of impact. These conditions were not necessary from a purely control point of view, but they allowed us to see more clearly the effects of our impact force reduction strategies on the joint motions during simulation.

The characteristics of the simulated three degrees-of-freedom manipulator used to test the strategy presented in this section are listed in Table 1. The impact event is pictured in Figure 3.

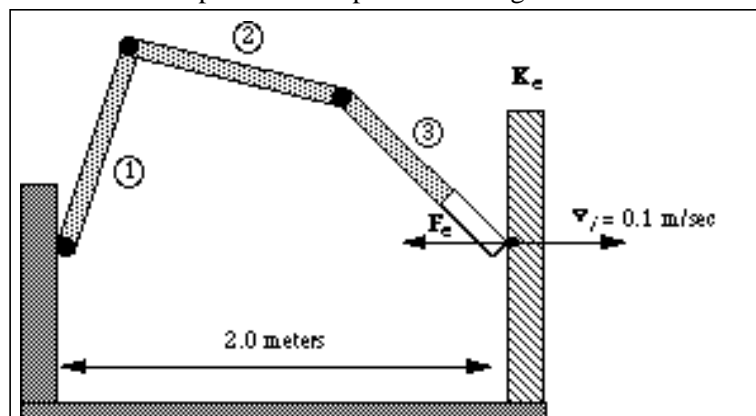


Figure 3: The impact event. The wall has a stiffness of $K_e = 100,000 \text{ n/m}$.

5.3. Testing the Impact Control Strategy

In the impact control strategy given in Section 3, we reduce the impact force experienced by the end-effector during a collision with an object by adding a damping torque to the joints, with the scalar h_1 controlling the amount of net torque and the scalar h_2 controlling the amount of null torque. We hypothesized that increasing the net torque would reduce penetration, while altering the amount of null torque added to the system should not significantly alter the penetration.

In our simulated three degrees-of-freedom planar manipulator, increasing h_1 caused the system to oscillate at a faster rate (without losing contact). At even higher values of h_1 , the end-effector stayed sunk into the surface. Figure 4 shows the simulated effect of several different values of h_1 on the impact response over time.

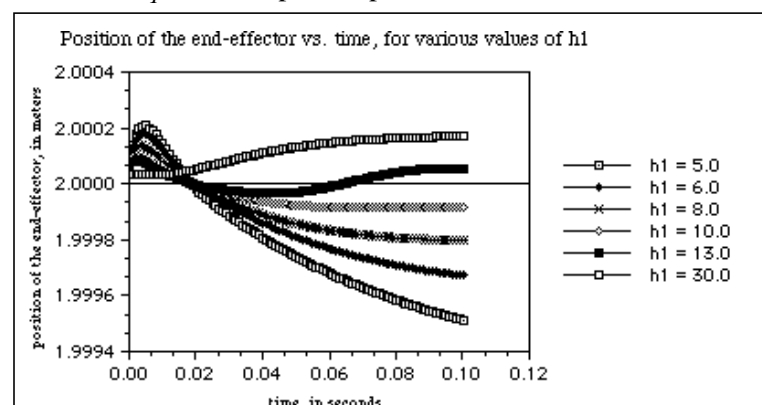


Figure 4: The position of the end-effector vs. time for several values of h_1 . $\theta = (60, -60, -60)$ degrees.

Increasing h_2 had very little effect on the impact force, since null motion does not drive the arm deeper into the surface, and since our null motion was very small relative to the net motion at the start of the impact event. The amount of penetration increased only slightly, even for extremely large values of h_2 , as shown in Figure 5. Similar in-

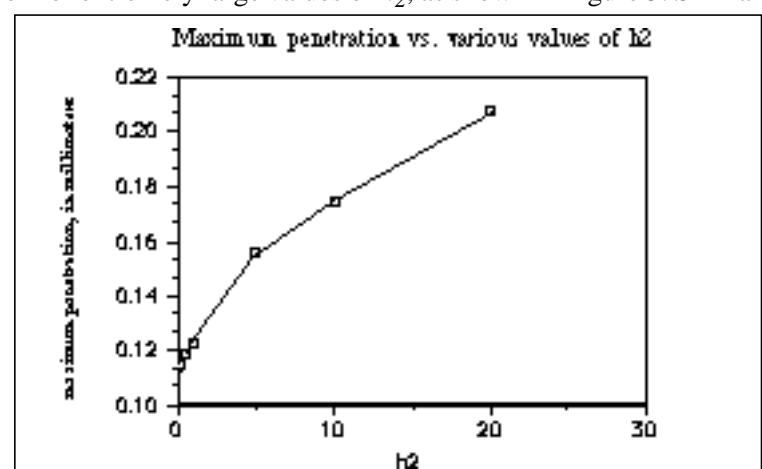


Figure 5: Penetration vs. several values of h_2 , for $\theta = (60, -60, -60)$ degrees and $h_1 = 10.0$.

creases and decreases in h_1 cause much more dramatic changes in the penetration, as shown in Figure 6. A small h_2 is desirable if we do not wish to damp null motion, and if we wish to allow more room for a large amount of net torque, keeping the saturation limits of the motors in mind.

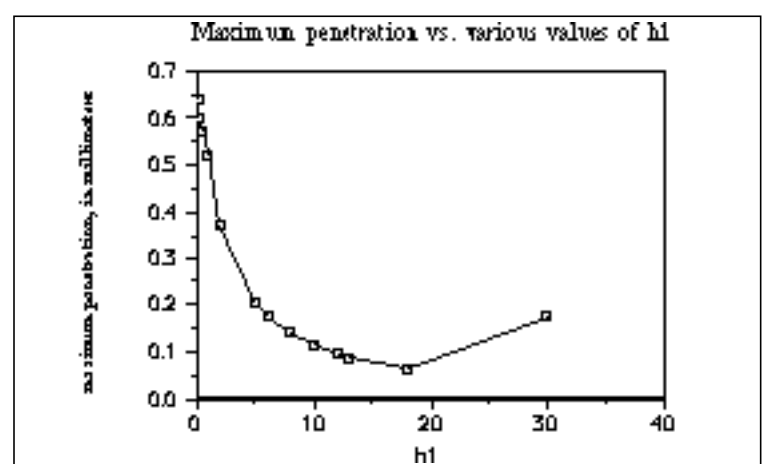


Figure 6: Penetration vs. several values of h_1 , for $\theta = (60, -60, -60)$ degrees and $h_2 = 0.01$. Note change of scale.

The results of our simulations clearly show that, for our simulated ideal three degrees-of-freedom planar manipulator, the impact

control strategy presented in Section 3 allows us to reduce the impact force between a manipulator and an object. These results are such that we feel we can conclude that this strategy would be effective for reducing the impact force for any actual redundant manipulator.

5.4. Testing the Impact Planner

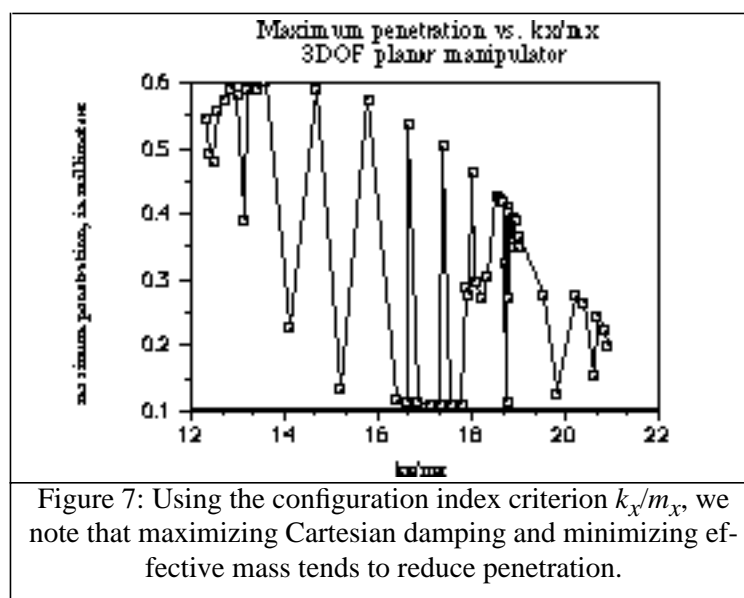
In the impact planner strategy given in Section 4, we reduce the impact force experienced by the end-effector during a collision with an object by choosing the configuration most suited to an impact event. We hypothesized that the configuration with the highest effective damping a_x should globally be the configuration with the least penetration. (We specify a global maximum because the effective mass also changes as the configuration changes. In our testing, this change in effective mass was not as radical as the change seen in the effective damping.)

A perhaps more intuitive criterion would be the ratio between the effective task-space damping and the effective mass:

$$K_T = (JK_D^{-1}J^T)^{-1} \quad (36)$$

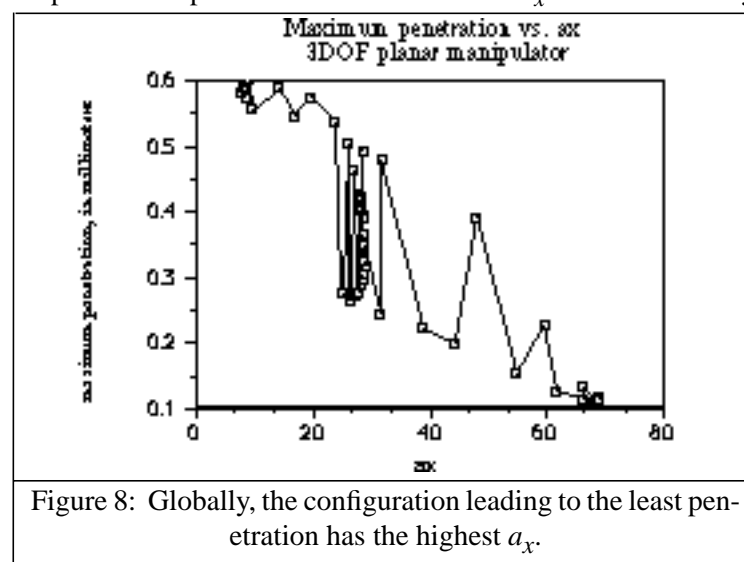
$$d_x = k_x/m_x = (u^T K_T u) / (u^T M u) \quad (37)$$

As can be seen in Figure 7, this criterion shows that minimizing the ef-



fective mass and maximizing the effective task-space damping reduces the penetration. However, it is difficult to pinpoint the best configuration from the use of this criteria, since the highest value of k_x/m_x does not quite correlate to the lowest value of penetration. To find the best configuration, we use a_x as the criteria.

Figure 8 shows a plot of penetration versus a_x for the simulated 3DOF planar manipulator. Different values of a_x were achieved by al-



tering the angle between the wall and the third link of the manipulator.

As hypothesized, the configuration having the highest effective damping is globally the configuration which yields the least penetration. (The bifurcation in these graphs comes from the fact that a three degrees-of-freedom planar manipulator can make contact with a surface at a particular angle in two ways: “elbow up” and “elbow down,” with either having different effective damping and effective mass characteristics.)

For our simulated ideal redundant manipulators, the strategy presented in this section allowed us to reduce the impact force between a manipulator and an object by changing the configuration of the manipulator in such a way that the effective damping is increased. From these simulation results, we conclude that this strategy would be effective for reducing the impact force for an actual redundant manipulator.

Summary

In this paper, we have presented and discussed two strategies for minimizing the force of impact event having some finite duration: an impact control strategy and an impact planner strategy, which were both derived by use of the Premultiplier Diagram. By applying the impact control strategy to a simulated redundant manipulator, we were able to minimize the force of the impact between an end-effector and an object by applying a damping torque at the time of impact. Our results suggest that net motion should be heavily damped, while null motion should not, in order that the actuators can be used to the best of their abilities. It was also seen in our simulations of the impact planner strategy that certain configurations were better at minimizing impact force than others, and the response of a particular configuration could be gauged by examining the effective damping of the system. Based on these simulation results, we conclude that the strategies presented in this paper would be effective at minimizing the force of impact on actual redundant manipulators.

References

- [1] C. Cai, *Instantaneous Robot Motion with Contact between Surfaces*, Ph.D. Thesis, Dept. of Computer Science, Stanford University, 1988.
- [2] J.J. Craig, *Introduction to Robotics: Mechanics and Control*, Addison-Wesley Publishing Company, Inc., Reading, Massachusetts, ©1989.
- [3] M.W. Gertz, “Simulation of Strategies to Minimize the Force of Impact Between a Redundant Manipulator and an Obstacle,” M.S. thesis, The Robotics Institute, Carnegie Mellon University, February 1991.
- [4] O. Khatib, “Dynamic Control of Manipulators in Operational Space,” Sixth CISM-IFTOMM Congress on Theory of Machines and Mechanisms, Dec. 1983, pp. 1128-1131, New Delhi, India (Wiley, New Delhi).
- [5] O. Khatib and J. Burdick, “Motion and Force Control of Robot Manipulators,” 1986 IEEE Conference on Robotics and Automation, San Francisco, CA, pp. 1381-1386, 1986.
- [6] J.O. Kim and P.K. Khosla, “Dynamic Resolution of Redundant Motions,” Technical Report CMU-RI-AML-90-01, Advanced Manipulators Laboratory, The Robotics Institute, Carnegie Mellon University, Sept. 1990.
- [7] J.O. Kim, P.K. Khosla, and W.K. Chung, “Static Modeling and Control of Redundant Manipulators,” *Journal of Robotic Systems*, 1991.
- [8] D.N. Nenchev, “Redundancy Resolution through Local Optimization: A Review,” *Journal of Robotic Systems* 6(6), pp. 769-798 (1989), John-Wiley & Sons, Inc., ©1989.
- [9] C.R. Rao and S.K. Mitra, *Generalized Inverse of Matrices and its Application*, John Wiley & Sons, Inc., ©1971.
- [10] I. D. Walker, “The Use of Kinematic Redundancy in Reducing Impact and Contact Effects in Manipulation,” 1990 IEEE Conference on Robotics and Automation, Cincinnati, OH, pp. 434-439, May 1990.
- [11] T. Yoshikawa, “Analysis and Control of Redundant Manipulators with Redundancy,” *Robotics Research: The first int. symp.*, ed. Brady and Paul, MIT press, pp. 735-747, 1984.
- [12] Y. Zheng and H. Hemami, “Mathematical Modeling of a Robot Collision with its Environment,” *Journal of Robotic Systems*, pp. 289-307, ©1985.
- [13] Y. Nakamura, *Advanced Robotics: Redundancy and Optimization*, Addison-Wesley Publishing Company, Inc., Reading, Massachusetts, ©1991.